

Microscopic quantum coherence in a photosynthetic-light-harvesting antenna

BY JAHAN M. DAWLATY¹, AKIHITO ISHIZAKI², ARIJIT K. DE^{1,3}
AND GRAHAM R. FLEMING^{1,3,*}

¹Department of Chemistry, University of California, Berkeley, CA 94720,
USA, ²Institute for Molecular Science, National Institutes of Natural Sciences,
Okazaki 444-8585, Japan, and ³Physical Biosciences Division, Lawrence
Berkeley National Laboratory, Berkeley, CA 94720, USA

We briefly review the coherent quantum beats observed in recent two-dimensional electronic spectroscopy experiments in a photosynthetic-light-harvesting antenna. We emphasize that the decay of the quantum beats in these experiments is limited by ensemble averaging. The *in vivo* dynamics of energy transport depends upon the local fluctuations of a single photosynthetic complex during the energy transfer time (a few picoseconds). Recent analyses suggest that it remains possible that the quantum-coherent motion may be robust under individual realizations of the environment-induced fluctuations contrary to intuition obtained from condensed phase spectroscopic measurements and reduced density matrices. This result indicates that the decay of the observed quantum coherence can be understood as ensemble dephasing. We propose a fluorescence-detected single-molecule experiment with phase-locked excitation pulses to investigate the coherent dynamics at the level of a single molecule without hindrance by ensemble averaging. We discuss the advantages and limitations of this method. We report our initial results on bulk fluorescence-detected coherent spectroscopy of the Fenna–Mathews–Olson complex.

Keywords: quantum coherence; photosynthesis; ensemble averaging; decoherence; two-dimensional electronic spectroscopy; single-molecule spectroscopy

1. Introduction

The photosynthetic conversion of the physical energy of sunlight into its chemical form suitable for cellular processes involves a variety of physical and chemical mechanisms [1–3]. Photosynthesis starts with the absorption of a photon of sunlight by one of the light-harvesting pigments, followed by transfer of the excitation energy to the reaction centre, where charge separation is initiated. At low light intensities, surprisingly, the quantum efficiency of the transfer is near unity—that is, each of the absorbed photons almost certainly reaches the reaction centre and drives the charge separation. A longstanding question in photosynthesis has been the following: how do light-harvesting systems

*Author for correspondence (grfleming@lbl.gov).

One contribution of 14 to a Theo Murphy Meeting Issue ‘Quantum-coherent energy transfer: implications for biology and new energy technologies’.

deliver such a high efficiency in the presence of a highly disordered and fluctuating dissipative environment? The molecular details of the initial stage of photosynthesis are not yet fully elucidated.

Great strides in femtosecond laser technology have opened up real-time observation of dynamical processes in complex chemical and biological systems. Recently, techniques of two-dimensional electronic spectroscopy [4] have been applied to explore photosynthetic-light-harvesting complexes and revealed the existence of long-lived quantum coherence among the electronic excited states of the multiple pigments in pigment–protein complexes (PPCs) [5]. Although the coherence in the PPCs was originally observed outside the physiological range of temperatures [5–7], recent experiments detected the presence of quantum coherence lasting up to approximately 300 fs even at physiological temperatures [8,9], which is consistent with a previous theoretical prediction [10]. These observations have led to the suggestion that quantum coherence might be vital in achieving the remarkable efficiency of photosynthetic light harvesting. With the general belief that biological organisms have adapted in the course of evolution so as to function most effectively in a given environment, a number of investigations were triggered to unlock the quantum secrets of photosynthetic light harvesting, e.g. the relevance, significance and universality of quantum coherence in photosynthesis [10–50]. Actually, it was demonstrated that strong quantum coherence can accelerate electronic energy transfer (EET) in certain circumstances [34,35] from the viewpoint of thermally activated barrier crossing. Essentially, the photosynthetic EET process is a kind of chemical reaction dynamics in condensed media, and therefore such traditional physico-chemical understandings should not be overlooked in order to obtain correct physical insights into these issues.

In this paper, we provide an overview of recent experimental and theoretical investigations of photosynthetic EET, specifically addressing the question of whether the decay of the coherent beating signal detected by means of two-dimensional electronic spectroscopy is due to true quantum mechanical decoherence or ensemble dephasing, which is also called ‘fake decoherence’ [51,52]. We propose a fluorescence-detected single-molecule coherent spectroscopy scheme for removing the effects of ensemble averaging from spectroscopic observations. We present our initial data for a bulk fluorescence-detected experiment as a first step towards the proposed goal.

2. Quantum-coherent beats detected in bulk nonlinear spectroscopic measurements: two-dimensional spectroscopy

To date, all reports of experimental observation of quantum coherence have been through using bulk nonlinear optical experiments, in particular two-dimensional electronic spectroscopy. This section has two purposes. First, we emphasize that the spatially phase-matched implementation of two-dimensional spectroscopy makes it inherently a bulk, ensemble-averaged technique and unscalable to the microscopic domain. Second, we point out that the decay of quantum beats within the excited states (as reported in recent experiments) is limited by ensemble averaging. Relating the observed oscillatory features in two-dimensional spectra to the microscopic *in vivo* function of a single complex requires careful considerations, which will be provided in §3.

We provide a brief review of two-dimensional spectroscopy, with particular emphasis on its ensemble-averaged nature. In the most common implementation of two-dimensional electronic spectroscopy, three laser pulses with separate spatial direction and variable delays are focused on to the sample. The electric field of the j th pulse with spatial direction k_j and delays t_j may be written as $E_j(r, t) = A(r, t - t_j)\{\exp(-i\omega t + k_j \cdot r) + \exp(+i\omega t - k_j \cdot r)\}$. The interference of the three pulses in the sample induces spatial polarization gratings with temporally evolving phases. The polarization grating corresponding to the three-pulse-dependent third-order nonlinear response has wavevectors $-k_s = \pm k_1 \pm k_2 \pm k_3$, where all permutations of the signs are possible. Each component of this grating emits a field in a corresponding direction in space. In two-dimensional spectroscopy, the signal radiated by the nonlinear polarization grating $-k_1 + k_2 + k_3$ is collected while varying pulse delays. Such phase matching by spatially extended polarization gratings is helpful in isolating the signal from a desired order of interaction. However, it necessitates an ensemble averaging over a large number of photosynthetic complexes, as polarization gratings are necessarily much larger than the wavelength of light. They are formed in the laser focal volume that is usually of the order of 30–100 μm wide and approximately 200 μm thick. For these polarization gratings to be meaningful, the density of photosynthetic complexes in the sample is kept high enough such that the optical properties of the sample are practically continuous.

Individual actions of the three pulses may be described as follows. The first pulse with wavevector k_1 creates a coherence (superposition) between the ground and excited states in all complexes throughout the sample. This coherence evolves temporally at the difference frequency between the ground and excited state for time τ . The phase of this coherence varies spatially across the sample as $k_1 \cdot r$. After time τ , a second pulse with wavevector k_2 interferes with this coherence throughout the sample. The result is a periodic modulation of populations between ground and excited states or a population grating across the sample with wavevector $-k_1 + k_2$. Since each pulse contains frequencies resonant with all transitions, all excited states in each complex are simultaneously prepared. Consequently, a more accurate description of the polarization is a grating of coherences *within* the excited state. This grating evolves for time T known as the waiting time. All recent reports of quantum coherence in photosynthetic complexes have been based on the phase evolution of the excited states during time T . Finally, the third pulse with wavevector k_3 interacts with the sample and converts the population grating into a ground-excited state coherence once again, which radiates a signal in the $k_s = -k_1 + k_2 + k_3$ direction as it evolves for time t . The frequency–frequency correlation between the last (emitting) coherences and first (excitation) coherences for a fixed T is represented in a two-dimensional spectrum.

It is clear from this description that the signal is always averaged over the macroscopic extent of the gratings. We consider the case where the sample consists of complexes with a static disorder of energy gaps between the ground and excited states (inhomogeneous distribution). For photosynthetic complexes, such a distribution exists because of static (slowly varying) local environments of pigments in their protein matrix. It is well known that two-dimensional spectroscopy is capable of separating the homogeneous (rapidly fluctuating)

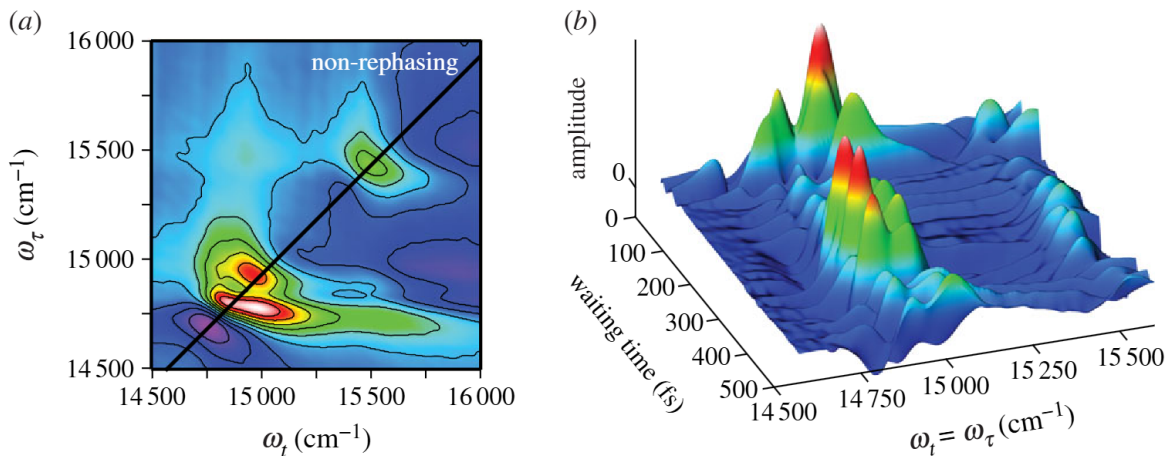


Figure 1. (a) The real part of the non-rephasing two-dimensional spectrum (waiting time $T = 250$ fs) of light-harvesting complex II (LHCII). (b) The amplitude of the diagonal cut of the non-rephasing two-dimensional spectra as a function of waiting time. For the purposes of presentation, a cubic spline interpolation connects the data points that were acquired in 10 fs increments. For (a,b), the amplitude increases from purple (negative) to white (positive). Adapted from Calhoun *et al.* [7]. (Online version in colour.)

distribution of energies from the inhomogeneous (static) distribution. With appropriate choices of relative delays of the excitation pulses, it is possible to measure only those components of the signal for which the phase evolution during τ and t occurs with opposite signs, resulting in cancellation of phase evolution owing to the static distribution. The corresponding signal is known as the rephasing, or photon-echo, signal.

Recent reports of long-lived electronic quantum coherence in photosynthetic complexes have been based on the evolution of coherences within the excited state during time T . When the evolution of two different states during T contributes to the same spectral feature in a two-dimensional spectrum, that feature will beat in amplitude as T is scanned. It is shown that such beats may be observed for both diagonal and off-diagonal peaks in non-rephasing and rephasing two-dimensional spectra, respectively [32], as shown in figure 1. We point out that, similar to the ground-excited state energy gaps, the energy gaps *within* the excited states also have a distribution. This time-dependent distribution contributes to the decay of the observed oscillations during time T .

In summary, two-dimensional spectroscopy studies the bulk nonlinear optical properties of a macroscopic sample of photosynthetic complexes. At least two conceptual links need to be made to relate these measured properties to the dynamics of an individual complex in a living organism. First, phase synchrony between spatially remote parts of the sample (i.e. polarization grating) is made possible by the large intensity and large spatial coherence length of laser light. Such synchrony is neither required for biological function nor possible in natural sunlight. Second, the effects of environmental fluctuations on spectroscopic measurements and on biological energy transport should be considered separately. The separation of energy variations into static (inhomogeneous) and dynamic (homogeneous) components is dictated by the restriction of the experimental method. Energy fluctuations are perceived as dynamic (or static) when the

spectroscopic measurement time is slower (or faster) than the time scale of fluctuation. Such experimentally dictated time scales do not have direct relevance to the *in vivo* function of a complex. The more relevant physiological time scale is that of excitation transport across the antenna to the reaction centre, which is of the order of a few picoseconds. The excitation experiences the environmental fluctuations over this transfer time scale only. Each new excitation experiences a different environmental Hamiltonian that determines its transport across the antenna. In light of these considerations, in the next section, we discuss the origins of the decay of oscillatory behaviour in bulk spectroscopic methods.

3. What are we seeing in the beats of two-dimensional electronic spectra?

Experimentally, as described in the preceding section, photosynthetic EET dynamics are investigated by synchronizing initial electronic excitation in the entire ensemble by means of ultrashort laser pulses. In natural-light harvesting, however, the initial event is the absorption of one sunlight photon by a single PPC, followed by EET in the PPC independently of the ensemble-averaged behaviour or our measurements.

One of the viable approaches to explore photosynthetic EET and to analyse condensed phase spectroscopic signals is a quantum master equation [2,53]. In this approach, one focuses attention only on the electronic excitation, which is termed the system, and treats the other degrees of freedom (DOFs) as the environment. The key quantity of interest is the reduced density matrix (RDM), i.e. the partial average of the total density matrix $\rho_{\text{tot}}(t)$ over the environmental DOFs:

$$\rho(t) = \text{Tr}_{\text{env}}[\rho_{\text{tot}}(t)]. \quad (3.1)$$

This matrix can be naturally introduced via the expectation value of a system's operator \mathcal{O}_{sys} as $\text{Tr}_{\text{tot}}[\mathcal{O}_{\text{sys}}\rho_{\text{tot}}(t)] = \text{Tr}_{\text{sys}}[\mathcal{O}_{\text{sys}}\rho(t)]$. For example, \mathcal{O}_{sys} is a transition dipole operator of a pigment when optical spectra are considered. In the literature of photosynthetic EET, the initial condition of the environmental DOFs is assumed to be the thermal equilibrium state $\rho_{\text{env}}^{\text{eq}}$, which is a mixed state, because of the lack of information on the environmental DOFs. Thus, the total density matrix is expressed as¹

$$\rho_{\text{tot}}(t) = e^{-iH_{\text{tot}}t/\hbar} [\rho_{\text{sys}}(0) \otimes \rho_{\text{env}}^{\text{eq}}] e^{iH_{\text{tot}}t/\hbar}, \quad (3.2)$$

with H_{tot} being the total Hamiltonian. This mixed-state density matrix formalism is employed to describe a true physical ensemble, i.e. a collection of multiple identical physical systems. Consequently, approaches of this type have a considerable domain of applicability in condensed phase chemical dynamics.

It is undeniable that the RDM approach based on equation (3.2) has provided useful insight into condensed phase spectra and photosynthetic EET. However, considering the difference between electronic excitation dynamics in individual PPCs and their ensemble average naturally raises the question as to whether such

¹The factorized initial condition of the form, $\rho_{\text{sys}}(0) \otimes \rho_{\text{env}}^{\text{eq}}$, is generally considered unphysical in the literature of open quantum systems because it neglects an inherent correlation between a system and its environment [54]. In electronic excitation processes, however, this initial condition is of no consequence because it corresponds to the electronic ground state or an electronic excited state generated by photoexcitation in accordance to the vertical Franck–Condon transition.

an approach might limit the understanding of the EET because the reduction procedure involves an ensemble average that may wash out the microscopic details. In particular, this issue becomes prominent when quantum coherence and its destruction are discussed. In the literature, descriptions of several different processes are sometimes referred to as ‘decoherence’. Most of these associations are based on the observation that different processes may all lead to the disappearance of off-diagonal elements in the density matrix of the system. Schlosshauer [52] describes ‘true decoherence’ and ‘fake decoherence’. According to Schlosshauer [52], true decoherence should be understood as a distinctly quantum mechanical effect with no classical analogue, independently of an ensemble average. When both the system and its environment are described quantum mechanically, the interaction between them leads to a quantum entangled state for the system–environment combination,

$$|\psi^{\text{tot}}(t)\rangle = \sum_n c_n(t) |\varphi_n^{\text{sys}}\rangle |\theta_n^{\text{env}}(t)\rangle, \quad (3.3)$$

where $|\varphi_n^{\text{sys}}\rangle$ is a system’s state in some basis and $|\theta_n^{\text{env}}(t)\rangle$ describes time-evolution of the environmental state associated with $|\varphi_n^{\text{sys}}\rangle$. This entanglement implies that the system and its environment share information on the system. However, measurements are usually performed only on the system, whereas the environment is typically either inaccessible or simply of no interest. Thus, the shared information is also inaccessible, and it means that a portion of the information on the system is lost as long as observers are able to measure only the observables that pertain to the system. This process corresponds to decoherence. Tracing over the inaccessible environmental states yields an RDM of the entangled subsystem as

$$\rho_{\text{reduced}}(t) = \sum_{mn} c_m(t) c_n^*(t) \langle \theta_m^{\text{env}}(t) | \theta_n^{\text{env}}(t) \rangle \cdot |\varphi_m^{\text{sys}}\rangle \langle \varphi_n^{\text{sys}}|. \quad (3.4)$$

Over time, an environmental state $|\theta_m^{\text{env}}(t)\rangle$ diverges maximally, and thus overlaps between the environmental states associated with the different $|\varphi_m^{\text{sys}}\rangle$ become small. Thus, the $\{|\theta_n^{\text{env}}(t)\rangle\}$ become mutually orthogonal, $\lim_{t \rightarrow \infty} \langle \theta_m^{\text{env}}(t) | \theta_n^{\text{env}}(t) \rangle = \delta_{mn}$, which results in the disappearance of the off-diagonal elements in equation (3.4) [52]. Following these lines of thought, the appearance of a classical world in quantum theory has been explored [51,52,55,56]. On the other hand, an example of fake decoherence is to interpret the result of an ensemble average over different noisy realizations of a system as the description of a decoherence process. As was mentioned earlier, the density matrix formalism is often used to describe a true physical ensemble, i.e. a collection of multiple physical systems in which each individual system is described by a pure state, $|\psi^{(n)}(t)\rangle$ [52]. In this situation, each system may start out in the same state but may be subject to slightly different Hamiltonians. For example, the Hamiltonian of each system may contain random fluctuations owing to the presence of classical noise. If we take the average over the ensemble $\{\psi^{(n)}(t)\}$ of the pure states of all N systems, the ensemble density matrix is obtained as

$$\rho_{\text{ensemble}}(t) = \frac{1}{N} \sum_{n=1}^N |\psi^{(n)}(t)\rangle \langle \psi^{(n)}(t)|. \quad (3.5)$$

In the limit of large N , the off-diagonal elements of the ensemble density matrix would disappear. This is evidently ensemble dephasing, not decoherence.

In principle, both the electronic excitations and the rest of the entire universe should be described quantum mechanically, as shown in equation (3.4). In practice, however, the protein environment embedding pigments are usually assumed to be classical objects and to induce classical noise in the electronic energies of the pigments. The statement that biological systems are ‘warm, wet and noisy environments’ is essentially a classical aspect of proteins, membranes and so on. Therefore, it is not obvious to what extent quantum features of the protein environment play a role in decoherence of electronic excitations. Also, it should be noted that equation (3.2) already involves a classical mixture in terms of the environmental DOFs prior to any reduction procedure, whereas equation (3.4) presents the so-called improper mixture [57] introduced by the reduction with respect to inaccessible environmental pure quantum states. Consequently, it is not obvious whether the decay of quantum-coherent beats observed in two-dimensional electronic spectra and calculated with the RDM based on equation (3.2) is describing decoherence or ensemble dephasing.

Recently, such a theoretical approach was examined [36] by employing a mixed quantum/classical simulation. A time-dependent self-consistent field approach was used [58–60]. In the approach, only the electronic excitation was treated quantum mechanically, while the environmental DOFs were described as classical variables. The combination of two fundamentally different descriptions of nature provided by quantum and classical mechanics might cause serious problems of consistency. In order to keep such contradictions to an acceptable level, it was assumed that the quantum mechanical action of the system on the environment could be ignored. The Hamiltonian for electronic excitations is time dependent because it contains random fluctuations due to the presence of classical noise. This assumption corresponds to stochastic approaches such as the temperature-independent Lindblad equation or the Haken–Strobl model [61], which are extensively employed for examining quantum effects in photosynthetic EET [11,18,20,21,38,39,42,43,62,63]. It should be noticed that the classical noise in this model forces the electronic excitation to remain in a pure quantum state, and therefore an ensemble dephasing effect can be discussed without any influence of decoherence. However, our purpose is not, of course, to deny that decoherence occurs; simply, we suggest that its time scale is not known.

In this paper, the Drude–Lorentz spectral density is assumed for the sake of simplicity, $\mathcal{J}_m(\omega) = 2\hbar\lambda_m\tau_m\omega/(\tau_m^2\omega^2 + 1)$, although arbitrary spectral densities can be employed for the present simulations. This density yields the correlation function of fluctuations in electronic energy of the m th pigment, $u_m(t)$, as

$$S_m(t) = \langle u_m(t)u_m(0) \rangle = 2\hbar\lambda_m k_B T \exp\left(-\frac{t}{\tau_m}\right), \quad (3.6)$$

where T , $\hbar\lambda_m$ and τ_m are the temperature, reorganization energy and relaxation time of the environment associated with the m th pigment, and k_B is the Boltzmann constant. We follow the discretization procedure of the spectral density described by Wang *et al.* [64], and employ 1000 phonon modes per site.

To simulate the EET dynamics of a monomeric subunit of the Fenna–Mathews–Olson (FMO) complex of *Chlorobaculum tepidum*, the spectral densities for the

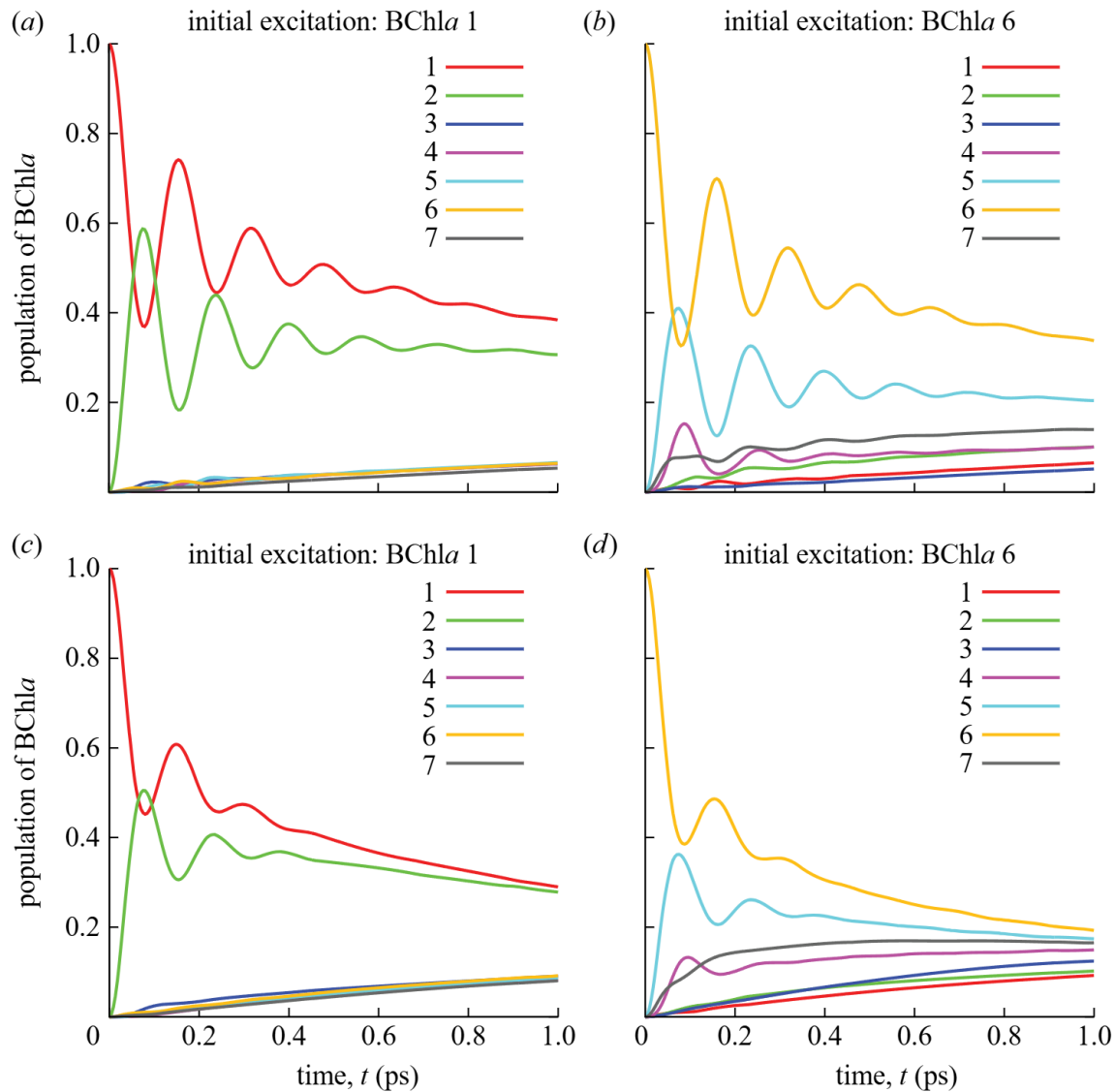


Figure 2. Ensemble-averaged time evolution of population of each BChla molecule in the FMO complex of *C. tepidum*. Calculations were performed from the mixed quantum/classical approach for cryogenic temperature 77 K (*a,b*) and physiological temperature 300 K (*c,d*). (Online version in colour.)

different sites are assumed to be equivalent, $\lambda_m \equiv \lambda = 35 \text{ cm}^{-1}$ and $\tau_m \equiv \tau = 100 \text{ fs}$; we use the Hamiltonian for the trimeric structure of the FMO complex obtained by Adolphs & Renger [65]. The FMO complex has been assumed to be oriented with BChla 1 and 6 towards the light-harvesting antenna, whereas BChla 3 and 4 define the target region in contact with the reaction centre complex [65,66]. Accordingly, we adopt BChla 1 or 6 as the initial excited pigment for numerical calculations.

Figure 2 shows ensemble-averaged excitation transfer dynamics calculated from the mixed quantum/classical approach. The statistical averages are taken for 50 000 realizations for the ensemble average. All the panels in figure 2 demonstrate that the ensemble average of pure-state quantum dynamics influenced by classical noise and the results of the reduced density matrices published in Ishizaki & Fleming [10] show excellent agreement in terms of quantum-coherent wave-like

behaviour. Quantum-coherent wave-like motion at 77 K is visible up to 700 fs, while it can be clearly observed up to 350 fs even at the physiological temperature, 300 K. However, a difference is observed in terms of the convergence in the longer time region; the reduced density matrices converge to the vicinity of the thermal equilibrium value, whereas the ensemble averages in figure 2 converge to $1/7 \approx 0.14$ corresponding to infinite temperature. This difference is explained as the breakdown of the fluctuation–dissipation relation in the mixed quantum/classical simulation in this work. In the quantum master equation approaches, the environmental correlation function $S_m(t)$ satisfies the fluctuation–dissipation relation with the environmental response function $\chi_m(t)$, which describes the environmental reorganization process. The fluctuation–dissipation relation is expressed as

$$\beta \frac{d}{dt} S_m(t) \simeq \chi_m(t) \quad (3.7)$$

in the classical limit, and guarantees that thermal equilibrium is reached at long times. In the present mixed quantum/classical simulation, however, we have assumed that the quantum mechanical action of the system on the environment could be ignored. This situation indicates that the environmental reorganization process is vanishing and correspondingly $\chi_m(t) = 0$. As the fluctuation–dissipation relation indicates, this situation corresponds to the infinite temperature limit, $\beta \rightarrow 0$. As a result, the ensemble averages of the present mixed quantum/classical trajectories converge to ‘the thermal equilibrium at the infinite temperature’. Recently, Kelly & Rhee [67] obtained a similar result by employing the quantum-classical Liouville equation [68] with the Poisson bracket mapping equation [69,70].

According to equation (3.6), the root mean square amplitude of the fluctuations in electronic energy of the m th pigment, $\delta\Omega_m$, can be estimated as

$$\hbar \cdot \delta\Omega_m = \sqrt{\langle u_m^2 \rangle} = \sqrt{2\hbar\lambda_m k_B T}. \quad (3.8)$$

With increasing reorganization energy λ and/or temperature T , therefore, the magnitude of the fluctuations increases.

Figure 3 presents the dephasing time of quantum coherence between delocalized excitons, $|e_1\rangle$ and $|e_2\rangle$, in the one-excitation manifold of a homodimer, as a function of (a) temperature T and (b) reorganization energy λ . Unless otherwise noted, we employ $J = 100 \text{ cm}^{-1}$, $\lambda = 50 \text{ cm}^{-1}$, $T = 300 \text{ K}$ and $\tau^{\text{rxn}} = 100 \text{ fs}$ as the default values. The dephasing times were determined as follows: we assume that site 1 is excited as an initial condition, and we calculate the time evolution of the ensemble behaviour. By transforming from the site representation to the exciton representation, we can obtain the time evolution of the coherence between the two excitons. From these data, we determine the dephasing time τ_D with a least-squares routine and a fitting function of $|\langle e_1 | \rho | e_2 \rangle| = 0.5 e^{-t/\tau_D}$. Reflecting the dependence of the root mean square amplitude of the pigments’ electronic energy fluctuations in equation (3.8), the dephasing time τ_D decreases with increasing temperature and reorganization energy. In this case, for a homodimer, the dependences of the dephasing time upon temperature and reorganization energy are nearly $\tau_D \propto T^{-1}$ and $\tau_D \propto \lambda^{-1}$. The pure dephasing model includes only those fluctuations whose amplitudes are expressed by equation (3.8), and therefore the role of temperature and that of

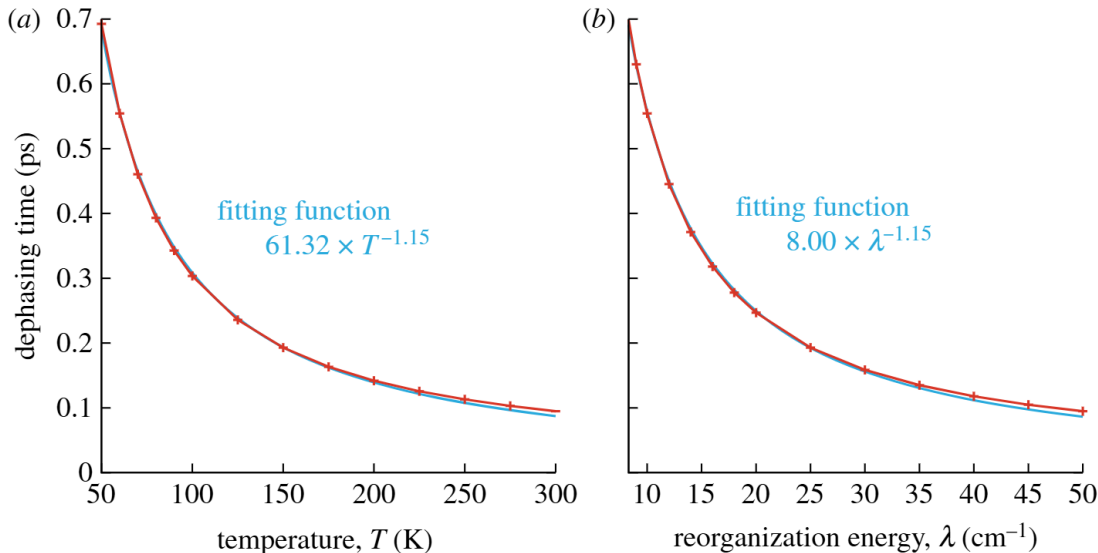


Figure 3. Dephasing time of quantum coherence between delocalized excitons, $|e_1\rangle$ and $|e_2\rangle$, in the one-excitation manifold of a homodimer, as a function of (a) temperature T with $\lambda = \lambda_m = 50\text{ cm}^{-1}$ and (b) reorganization energy λ with $T = 300\text{ K}$. We set $J_{12} = 100\text{ cm}^{-1}$ and $\tau^{\text{rxn}} = \tau_m^{\text{rxn}} = 100\text{ fs}$, as the default values. (Online version in colour.)

reorganization energy are the same as each other. We do not think that the exact value of the non-integral index, -1.15 , is physically important; time evolution of coherence between delocalized excitons is coupled to the excitons' population dynamics and is non-Markovian, and hence their dynamics is not necessarily characterized by exponential decay functions.

These discussions demonstrate that the decay of the observed coherent beats observed in two-dimensional electronic spectra of photosynthetic systems may be understood as the ensemble-averaged behaviours of the quantum dynamics of electronic excitation, rather than the quantum decoherence process [36].

4. Fluorescence-detected single-molecule coherent spectroscopy

In order to experimentally tackle the issues addressed in the preceding section, it is intriguing to explore the dynamics of electronic excitation wavepackets in a single photosynthetic PPC. Studying the slow spectral fluctuations of a single PPC is already achievable [71,72]. It has become possible to merge ultrafast spectroscopy and single-molecule detection [73–76]. Brinks *et al.* [75] reported the observation of vibrational wavepackets in individual molecules at ambient temperature by means of the phase-locked spontaneous light emission technique. In the early 1990s, this technique was originally employed for exploring vibrational wavepacket interferometry on an excited state potential surface of the iodine molecule in the gas phase [77,78]. Some of the conceptual foundations of this technique may be found in the study of Mukamel [79]. Applications of this technique to detection of electronic coherence in PPCs would provide further insights into photosynthetic EET and are currently in progress in our laboratory. Bulk fluorescence-based coherent multi-dimensional spectroscopy techniques have already been successfully applied to simple systems such as hot atomic Rb gas [80,81]. Fluorescence-based coherent multi-dimensional spectroscopy of a single

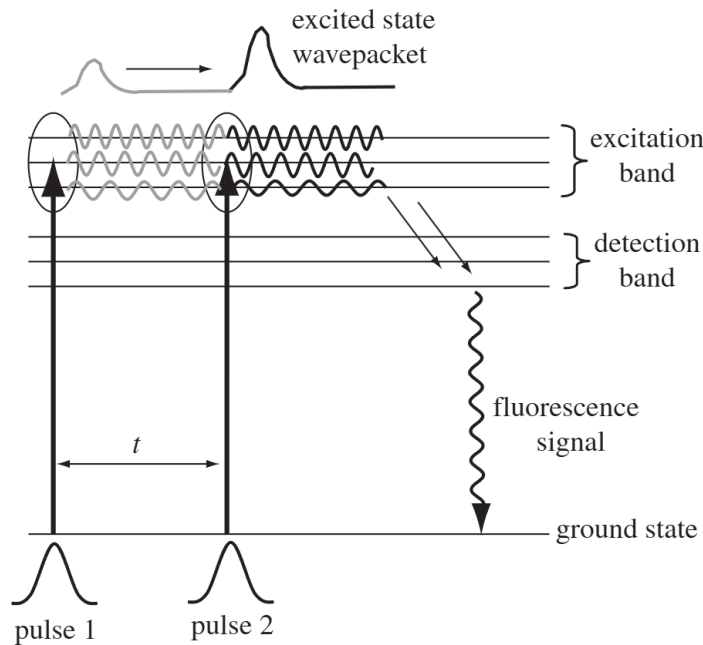


Figure 4. A schematic of fluorescence-detected electronic wavepacket interferometry. Two optical pulses have a fixed phase relation to each other and are resonant only with the excitation band of the sample. The first pulse prepares an electronic wavepacket (grey lines) that propagates in the excited state for time t . The second pulse excites a second wavepacket that interferes with the first one. The constructive/destructive interference of the two wavepackets determines the net population of the excited state, which can be measured as incoherent fluorescence after relaxation into the detection band. Oscillation of fluorescence yield as a function of delay time t indicates coherent evolution of the first wavepacket.

molecule has been recently studied theoretically [82]. In this section, we show that a single-molecule fluorescence experiment removes at least one layer of ambiguity, namely ensemble averaging, from the correct understanding of dynamics of excitation in a PPC.

Here, we discuss two schemes for fluorescence-detected coherent spectroscopy (FDCS). The first scheme is a two-pulse technique and is sensitive to the optical coherence between ground and excited states. As will be discussed, the information retrieved from this technique is effectively equivalent to the linear response of the single molecule. In the second scheme, fluorescence is detected as a function of the relative phases and delays of four phase-locked pulses. As will be discussed, the four-pulse scheme allows us to study coherences *within* the excited states of a photosynthetic complex.

(a) Two-pulse fluorescence-detected coherent spectroscopy

The scheme for the experiment is shown in figure 4. We separate the linear absorption spectrum of the antenna into two regions—the excitation band at the higher energy end and a detection band at the lower energy end of the spectrum. A short pulse that is resonant only with the high-energy region of the spectrum is delivered to the complex, which will prepare a superposition of electronic states between ground and excited states. Because many excited states are accessed by the pulse, the overall excitation may be referred to as an

electronic wavepacket, in analogy to the impulsively excited vibrational wavepackets [77,78] in molecular systems. However, in contrast to vibrational wavepackets, where many vibrational eigenstates are simultaneously accessed, here many electronic states in the excitation band are simultaneously excited. After the pulse, each electronic state acquires a phase proportional to its energy $\phi(t) = -(i/\hbar)(\tilde{E} + \int_0^t dt' \delta E(t'))$, where \tilde{E} is the average energy and $\delta E(t)$ is the environmentally induced stochastic fluctuations of energy. After a delay time τ , another short pulse with fixed phase relative to the first one interacts with the sample. The action of the second pulse may be described as launching a second wavepacket, which interferes with the first one. The net population of the excited state after the second pulse is determined by the interference of the two wavepackets. This population eventually relaxes to the detection band and can be measured as incoherent fluorescence. As the delay between the two pulses is scanned, the two wavepackets will undergo constructive/destructive interference leading to oscillating populations and consequently oscillating fluorescence yield as a function of delay. To further ensure the dependence of fluorescence yield on the relative phases of two pulses, a phase-cycling scheme may be employed.

Figure 5a shows the double-sided Feynman diagram corresponding to the two-pulse FDCS. As shown in the figure, the two-pulse FDCS is sensitive to the coherences between the ground and the excited states. Evolution of the $|g\rangle\langle e_1|$ and $|g\rangle\langle e_2|$ coherences during time τ results in rapid oscillations of the fluorescence yield at optical frequencies. Fourier transformation of the oscillations will correspond to the linear absorption spectrum of the system. The information content of a two-pulse FDCS is thus equivalent to that of the linear response of a single molecule. Because conventional measurement of the linear absorption spectrum of a single molecule is experimentally very difficult, a two-pulse FDCS or a frequency domain equivalent to it is valuable for recovering the $|g\rangle\langle e|$ dynamics of a single photosynthetic complex.

For a single photosynthetic PPC, it is necessary to average the measurement over many iterations (e.g. many laser pulses) owing to the inherent quantized nature of light emission from a single complex. The repetition rate of the experiment (number of laser pulses) cannot be increased beyond the fluorescence lifetime of a complex (a few nanoseconds). With fast repetition rate lasers (approx. 80 MHz), the averaging time of many seconds is typical for single-molecule experiments. Such long averaging time prevents us from observing a single realization of stochastic energy fluctuation and the corresponding energy transfer trajectory. In each experimental iteration, a new realization of the stochastic part of energy $\delta E(t)$ determines the outcome of wavepacket interference. Whether interference effects will persist upon averaging will be dictated by comparing the time scale of energy fluctuations with the experimental averaging time. The decay of oscillatory components of fluorescence indicates loss of phase relation between the initial and final excitations averaged over the measurement time.

It is clear that single-molecule spectroscopy avoids ensemble averaging, but does not avoid averaging the dynamics over measurement time. Despite this limitation, single-molecule spectroscopy still carries valuable information about the photosynthetic PPCs that is otherwise masked in a bulk experiment. This advantage is particularly distinct when the ensemble members are spread over a static distribution of energies.

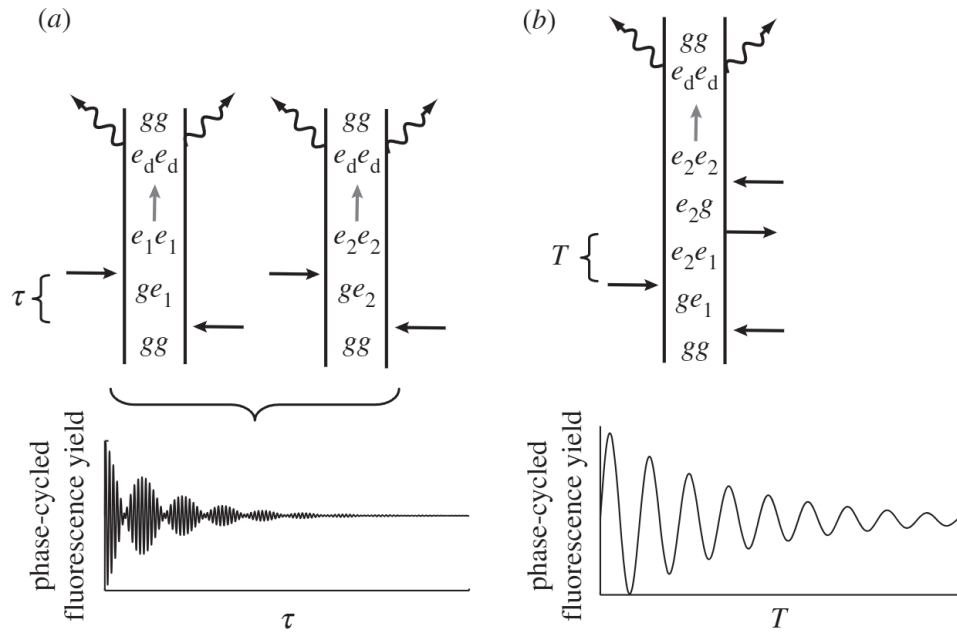


Figure 5. (a) Double-sided Feynman diagrams for a two-pulse FDCS experiment on a three-level system. Time runs from the bottom to the top. Straight black arrows show interaction with laser pulses, straight grey arrows show decay of population to the detection band and squiggly arrows indicate fluorescence emission. As τ is scanned, the phase-dependent portion of fluorescence shows rapid oscillation owing to the fast phase evolution of the $|g\rangle\langle e_1|$ and $|g\rangle\langle e_d|$ coherences. Beats are due to the interference of the two diagrams and the decay is due to the gap fluctuations. (b) A representative double-sided Feynman diagram for the four-pulse FDCS. The first two pulses generate a $|e_2\rangle\langle e_1|$ coherence between the excited states, which evolve for time T . The third and fourth pulses convert this coherence to an excited state population, which relaxes to the detection band and is measured as fluorescence. As time T is scanned, the phase-cycled fluorescence will oscillate at different frequencies between the $|e_1\rangle$ and $|e_2\rangle$ states, and will decay with a time scale proportional to the excited state energy gap fluctuations.

At room temperature, the fluctuations $\delta E(t)$ over the experimental integration time (approx. 1 s) may be too large for interference effects to survive. The experiment can be performed at cryogenic temperatures to reduce environmental fluctuations. As mentioned earlier, *in vivo* an excitation experiences fluctuations corresponding to physiological temperature over a relatively fast (few picoseconds) transfer time. In a time-averaged cryogenic experiment, the magnitude of fluctuations is reduced but they are averaged over a longer time. These two situations are not identical, as experiencing a hot environment for a short time, in general, is not the same as experiencing a cold environment for a long time. More theoretical and experimental investigations will be necessary to bridge the gap between the fluorescence-detected single-molecule wavepacket interferometry experiments and biological functions.

(b) Four-pulse fluorescence-detected coherent spectroscopy

The goal of a four-pulse FDCS experiment is to measure the coherence time *within* the excited states. The concept for the experiment is described in figure 5b. Four phase-locked pulses interact with the sample. The first two pulses generate between the two excited states ($|e_2\rangle\langle e_1|$ coherence) a coherence that evolves for

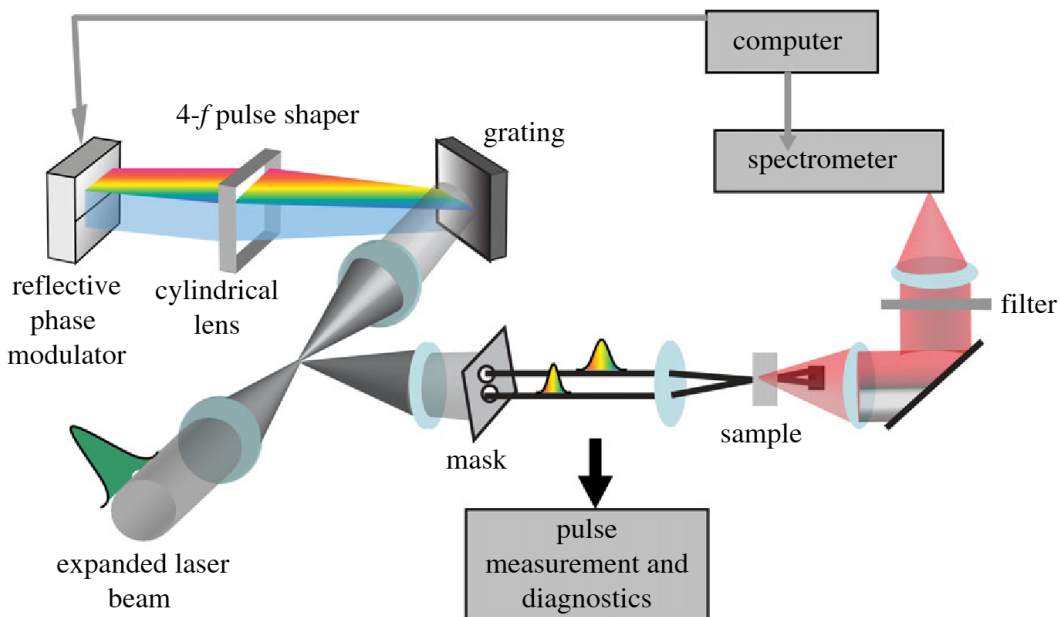


Figure 6. A diagram of the apparatus used for bulk FDCS. An expanded laser beam is sent through a 1:1 telescope to a 4-*f* pulse shaper with a two-dimensional liquid crystal reflective phase modulator. Two regions of the phase modulator are dedicated for delaying and shaping the two pulses needed for the experiment, which are reflected and retrieved with a pick-off mirror. A spatial mask is used to isolate the two beams. After focusing on the sample with a shallow angle, the beams are blocked and the fluorescence in the forward direction is collected, filtered and guided to a spectrometer. Phase-dependent fluorescence is measured as a function of the relative delay of the two pulses. (Online version in colour.)

time T . The third and fourth pulses convert this coherence to an excited state population, which relaxes to the detection band and is measured as fluorescence. A $2^4 = 16$ phase cycle scheme can isolate the component of fluorescence that depends on the phases of all pulses. The utility of phase cycling to isolate various third-order nonlinear optical pathways has been demonstrated previously [80,81,83–86]. As time T is scanned, the phase-cycled fluorescence will oscillate at different frequencies between the states $|e_1\rangle$ and $|e_2\rangle$. The decay of the oscillation will be determined by the fluctuations of the energy gap between the $|e_1\rangle$ and $|e_2\rangle$ states. In this case, unlike the conventional implementation of two-dimensional spectroscopy, the decay of the $|e_1\rangle$ and $|e_2\rangle$ coherence will not be limited by ensemble averaging over a large distribution of $|e_2\rangle\langle e_1|$ frequencies.

(c) Initial results for bulk fluorescence-detected coherent spectroscopy of Fenna–Mathews–Olson

In this section, we present our initial results on bulk two-pulse FDCS of FMO. The experiment is carried out using a multi-purpose coherent multi-dimensional spectroscopy apparatus based on the designs in the study of Gundogdu *et al.* [87] and Dawlaty *et al.* [88]. The configuration used for the fluorescence experiment is shown in figure 6. Delay and phase control of the two pulses is performed with a liquid crystal two-dimensional phase modulator in a 4-*f* pulse shaper geometry. The two pulses are focused on a 200 μm thick film of FMO in buffer and glycerol. The sample is kept at 77 K temperature in a liquid nitrogen cryostat. Fluorescence

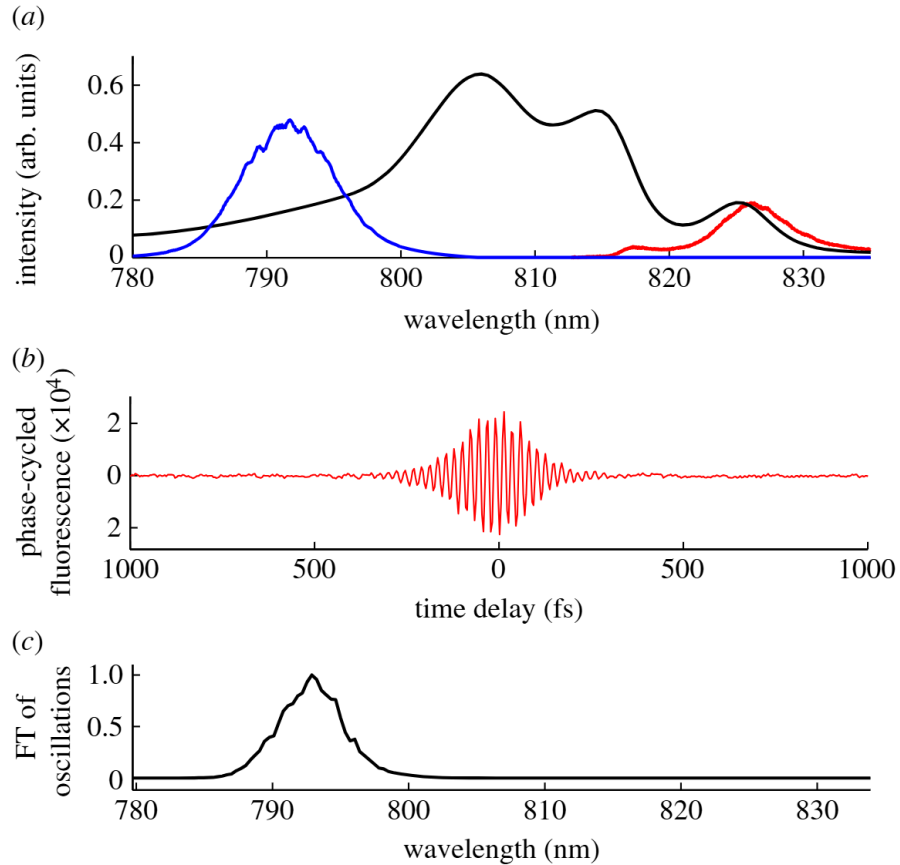


Figure 7. Initial results for FDGS of FMO. (a) The linear absorption spectrum of FMO (black) along with the spectrum of excitation pulses (blue) and the fluorescence spectrum (red) emerging at the frequency of the lowest energy exciton. (b) Phase-dependent fluorescence yield near 826 nm as a function of delay between the two phase-locked excitation pulses. The frequency of oscillations is lowered by a choice of rotating frame for reduced sampling. (c) Power spectrum of fluorescence oscillations. (Online version in colour.)

from the sample is collected in the forward direction after blocking the excitation beams. A long-pass filter with a cut-off wavelength of 815 nm is used to isolate the fluorescence.

The spectrum of excitation pulses and fluorescence overlaid on the absorption spectrum are shown in figure 7a. The excitation spectrum overlaps with the higher energy end of the absorption spectrum and corresponds to a pulse of about 110 fs in the time domain. The fluorescence spectrum has a peak at the lowest energy exciton of the complex and exhibits the typical Stokes shift of about 1.5 nm. The phase-cycled fluorescence signal S_{PC} is defined as

$$S_{PC} = S(\Delta\phi = 0) - S(\Delta\phi = \pi), \quad (4.1)$$

where $S(\Delta\phi = 0)$ and $S(\Delta\phi = \pi)$ are the fluorescence signals when the relative constant phase difference $\Delta\phi$ between the two pulses is 0 and π , respectively. The pulse shaper allows us to execute pulse delays with respect to a rotating frame [86] for reducing the sampling rate along the delay axis. The phase-cycled fluorescence signal integrated over a narrow spectral region near the peak of fluorescence is shown in figure 7b. The fluorescence yield as a function of delay exhibits oscillatory behaviour in the pulse overlap region. The oscillations occur

at approximately 2.6 fs, corresponding to the optical frequency of the excited energy levels. However, because of the choice of the rotating frame for reduced sampling of the delay range the oscillations appear at approximately 23 fs. The power spectrum of oscillations, after the appropriate shift for the rotating frame frequency, is shown in figure 7b.

As expected for a bulk sample with inhomogeneously distributed energy levels, the oscillations persist only under pulse overlap. Fourier transform of the oscillations leads to a spectrum that is almost identical to the excitation pulse. The slight shift of the power spectrum of fluorescence oscillations with respect to the excitation pulse may be due to the rising linear absorption from the blue to the red end of the excitation pulse. We are working on extending this experiment in two directions. First, the excitation pulse bandwidth should be increased to cover a larger range of the linear absorption spectrum. Second, the sample should be a single photosynthetic complex where the linear absorption line-width and corresponding fluorescence oscillations are not limited by the inhomogeneous distribution of energies. Furthermore, with our current apparatus, extension of this method to four-pulse FDCS and phase-cycled collection of signal from a single photosynthetic complex should be feasible.

5. Concluding remarks

In this work, we have discussed the ensemble-averaged nature of two-dimensional spectroscopy, which has been used to study coherent dynamics of excitations in a photosynthetic antenna. We have emphasized that decay of oscillations of spectral features as a function of the waiting time T is determined by ensemble averaging. Linking such spectroscopic observations to the physiological function of light harvesting requires careful analysis. Our theoretical analysis suggests that it remains possible that the quantum-coherent motion may be robust under individual realizations of the environment-induced fluctuations, contrary to intuition obtained from condensed phase spectroscopic measurements and reduced density matrices, indicating that the decay of the observed quantum coherence can be understood as ensemble dephasing. We have proposed fluorescence-detected single-molecule wavepacket interferometry as a new experimental direction for studying quantum-coherent effects without hindrance by ensemble averaging. We have discussed the advantages and limitations of this method. We have presented initial data for bulk FDCS of FMO. We anticipate that extension of this method to a single molecule can bring us closer to understanding the physiological significance of quantum coherence in light harvesting.

This work was supported by the Director, Office of Science, Office of Basic Energy Sciences, of the US Department of Energy under contract DE-AC02-05CH11231, by the Chemical Sciences, Geosciences and Biosciences Division, Office of Basic Energy Sciences, US Department of Energy, under contract DE-AC03-76SF000098 and by DARPA under grant no. N66001-09-1-2026. J.M.D. was supported by the QB3 distinguished post-doctoral fellowship from the California Institute of Quantitative Biosciences.

References

- 1 Hall, D. O. & Rao, K. K. 1999 *Photosynthesis*, 6th edn. Cambridge, UK: Cambridge University Press.

- 2 van Amerongen, H., Valkunas, L. & van Grondelle, R. 2000 *Photosynthetic excitons*. Singapore: World Scientific.
- 3 Blankenship, R. E. 2002 *Molecular mechanisms of photosynthesis*. Oxford, UK: Blackwell Science.
- 4 Cho, M. 2009 *Two-dimensional optical spectroscopy*. Boca Raton, FL: CRC Press.
- 5 Engel, G. S., Calhoun, T. R., Read, E. L., Ahn, T.-K., Mančal, T., Cheng, Y.-C., Blankenship, R. E. & Fleming, G. R. 2007 Evidence for wavelike energy transfer through quantum coherence in photosynthetic systems. *Nature* **446**, 782–786. ([doi:10.1038/nature05678](https://doi.org/10.1038/nature05678))
- 6 Lee, H., Cheng, Y.-C. & Fleming, G. R. 2007 Coherence dynamics in photosynthesis: protein protection of excitonic coherence. *Science* **316**, 1462–1465. ([doi:10.1126/science.1142188](https://doi.org/10.1126/science.1142188))
- 7 Calhoun, T. R., Ginsberg, N. S., Schlau-Cohen, G. S., Cheng, Y.-C., Ballottari, M., Bassi, R. & Fleming, G. R. 2009 Quantum coherence enabled determination of the energy landscape in light-harvesting complex II. *J. Phys. Chem. B* **113**, 16 291–16 295. ([doi:10.1021/jp908300c](https://doi.org/10.1021/jp908300c))
- 8 Collini, E., Wong, C. Y., Wilk, K. E., Curmi, P. M. G., Brumer, P. & Scholes, G. D. 2010 Coherently wired light-harvesting in photosynthetic marine algae at ambient temperature. *Nature* **463**, 644–648. ([doi:10.1038/nature08811](https://doi.org/10.1038/nature08811))
- 9 Panitchayangkoon, G., Hayes, D., Fransted, K. A., Caram, J. R., Harel, E., Wen, J., Blankenship, R. E. & Engel, G. S. 2010 Long-lived quantum coherence in photosynthetic complexes at physiological temperature. *Proc. Natl Acad. Sci. USA* **107**, 12 766–12 770. ([doi:10.1073/pnas.1005484107](https://doi.org/10.1073/pnas.1005484107))
- 10 Ishizaki, A. & Fleming, G. R. 2009 Theoretical examination of quantum coherence in a photosynthetic system at physiological temperature. *Proc. Natl Acad. Sci. USA* **106**, 17 255–17 260. ([doi:10.1073/pnas.0908989106](https://doi.org/10.1073/pnas.0908989106))
- 11 Olaya-Castro, A., Lee, C. F., Olsen, F. F. & Johnson, N. F. 2008 Efficiency of energy transfer in a light-harvesting system under quantum coherence. *Phys. Rev. B* **78**, 085115. ([doi:10.1103/PhysRevB.78.085115](https://doi.org/10.1103/PhysRevB.78.085115))
- 12 Nazir, A. 2009 Correlation-dependent coherent to incoherent transitions in resonant energy transfer dynamics. *Phys. Rev. Lett.* **103**, 146404. ([doi:10.1103/PhysRevLett.103.146404](https://doi.org/10.1103/PhysRevLett.103.146404))
- 13 Fassioli, F., Nazir, A. & Olaya-Castro, A. 2010 Quantum state tuning of energy transfer in a correlated environment. *J. Phys. Chem. Lett.* **1**, 2139–2143. ([doi:10.1021/jz100717d](https://doi.org/10.1021/jz100717d))
- 14 Jang, S., Cheng, Y.-C., Reichman, D. R. & Eaves, J. D. 2008 Theory of coherent resonance energy transfer. *J. Chem. Phys.* **129**, 101104. ([doi:10.1063/1.2977974](https://doi.org/10.1063/1.2977974))
- 15 Jang, S. 2009 Theory of coherent resonance energy transfer for coherent initial condition. *J. Chem. Phys.* **131**, 164101. ([doi:10.1063/1.3247899](https://doi.org/10.1063/1.3247899))
- 16 Mohseni, M., Rebentrost, P., Lloyd, S. & Aspuru-Guzik, A. 2008 Environment-assisted quantum walks in photosynthetic energy transfer. *J. Chem. Phys.* **129**, 174106. ([doi:10.1063/1.3002335](https://doi.org/10.1063/1.3002335))
- 17 Rebentrost, P., Mohseni, M. & Aspuru-Guzik, A. 2009 Role of quantum coherence and environmental fluctuations in chromophoric energy transport. *J. Phys. Chem. B* **113**, 9942–9947. ([doi:10.1021/jp901724d](https://doi.org/10.1021/jp901724d))
- 18 Rebentrost, P., Mohseni, M., Kassal, I., Lloyd, S. & Aspuru-Guzik, A. 2009 Environment-assisted quantum transport. *New J. Phys.* **11**, 033003. ([doi:10.1088/1367-2630/11/3/033003](https://doi.org/10.1088/1367-2630/11/3/033003))
- 19 Rebentrost, P., Chakraborty, R. & Aspuru-Guzik, A. 2009 Non-markovian quantum jumps in excitonic energy transfer. *J. Chem. Phys.* **131**, 184 102–184 109. ([doi:10.1063/1.3259838](https://doi.org/10.1063/1.3259838))
- 20 Plenio, M. B. & Huelga, S. F. 2008 Dephasing-assisted transport: quantum networks and biomolecules. *New J. Phys.* **10**, 113019. ([doi:10.1088/1367-2630/10/11/113019](https://doi.org/10.1088/1367-2630/10/11/113019))
- 21 Caruso, F., Chin, A. W., Datta, A., Huelga, S. F. & Plenio, M. B. 2009 Highly efficient energy excitation transfer in light-harvesting complexes: the fundamental role of noise-assisted transport. *J. Chem. Phys.* **131**, 105106. ([doi:10.1063/1.3223548](https://doi.org/10.1063/1.3223548))
- 22 Caruso, F., Chin, A. W., Datta, A., Huelga, S. F. & Plenio, M. B. 2010 Entanglement and entangling power of the dynamics in light-harvesting complexes. *Phys. Rev. A* **81**, 062346. ([doi:10.1103/PhysRevA.81.062346](https://doi.org/10.1103/PhysRevA.81.062346))
- 23 Chin, A. W., Datta, A., Caruso, F., Huelga, S. F. & Plenio, M. B. 2010 Noise-assisted energy transfer in quantum networks and light-harvesting complexes. *New J. Phys.* **12**, 065002. ([doi:10.1088/1367-2630/12/6/065002](https://doi.org/10.1088/1367-2630/12/6/065002))

- 24 Abramavicius, D., Voronine, D. V. & Mukamel, S. 2008 Unravelling coherent dynamics and energy dissipation in photosynthetic complexes by 2D spectroscopy. *Biophys. J.* **94**, 3613–3619. (doi:10.1529/biophysj.107.123455)
- 25 Palmieri, B., Abramavicius, D. & Mukamel, S. 2009 Lindblad equations for strongly coupled populations and coherences in photosynthetic complexes. *J. Chem. Phys.* **130**, 204512. (doi:10.1063/1.3142485)
- 26 Mukamel, S. 2010 Signatures of quasiparticle entanglement in multidimensional nonlinear optical spectroscopy of aggregates. *J. Chem. Phys.* **132**, 241105. (doi:10.1063/1.3454657)
- 27 Thorwart, M., Eckel, J., Reina, J. H., Nalbach, P. & Weiss, S. 2009 Enhanced quantum entanglement in the non-Markovian dynamics of biomolecular excitons. *Chem. Phys. Lett.* **478**, 234–237. (doi:10.1016/j.cplett.2009.07.053)
- 28 Nalbach, P., Eckel, J. & Thorwart, M. 2010 Quantum coherent biomolecular energy transfer with spatially correlated fluctuations. *New J. Phys.* **12**, 065043. (doi:10.1088/1367-2630/12/6/065043)
- 29 Womick, J. M. & Moran, A. M. 2009 Exciton coherence and energy transport in the light-harvesting dimers of allophycocyanin. *J. Phys. Chem. B* **113**, 15 747–15 759. (doi:10.1021/jp907644h)
- 30 Womick, J. M. & Moran, A. M. 2009 Nature of excited states and relaxation mechanisms in C-phycocyanin. *J. Phys. Chem. B* **113**, 15 771–15 782. (doi:10.1021/jp908093x)
- 31 Cheng, Y.-C., Engel, G. S. & Fleming, G. R. 2007 Elucidation of population and coherence dynamics using cross-peaks in two-dimensional electronic spectroscopy. *Chem. Phys.* **341**, 285–295. (doi:10.1016/j.chemphys.2007.07.049)
- 32 Cheng, Y.-C. & Fleming, G. R. 2008 Coherence quantum beats in two-dimensional electronic spectroscopy. *J. Phys. Chem. A* **112**, 4254–4260. (doi:10.1021/jp7107889)
- 33 Ishizaki, A. & Fleming, G. R. 2009 On the adequacy of the Redfield equation and related approaches to the study of quantum dynamics in electronic energy transfer. *J. Chem. Phys.* **130**, 234110. (doi:10.1063/1.3155214)
- 34 Ishizaki, A. & Fleming, G. R. 2009 Unified treatment of quantum coherent and incoherent hopping dynamics in electronic energy transfer: reduced hierarchy equation approach. *J. Chem. Phys.* **130**, 234111. (doi:10.1063/1.3155372)
- 35 Ishizaki, A. & Fleming, G. R. 2010 Quantum superpositions in photosynthetic light harvesting: delocalization and entanglement. *New J. Phys.* **12**, 055004. (doi:10.1088/1367-2630/12/5/055004)
- 36 Ishizaki, A. & Fleming, G. R. 2011 On the interpretation of quantum coherent beats observed in two-dimensional electronic spectra of photosynthetic light harvesting complexes. *J. Phys. Chem. B* **115**, 6227–6233. (doi:10.1021/jp112406h)
- 37 Sarovar, M., Ishizaki, A., Fleming, G. R. & Whaley, K. B. 2010 Quantum entanglement in photosynthetic light-harvesting complexes. *Nat. Phys.* **6**, 462–467. (doi:10.1038/nphys1652)
- 38 Sarovar, M., Cheng, Y.-C. & Whaley, K. B. 2011 Environmental correlation effects on excitation energy transfer in photosynthetic light harvesting. *Phys. Rev. E* **83**, 011906. (doi:10.1103/PhysRevE.83.011906)
- 39 Hoyer, S., Sarovar, M. & Whaley, K. B. 2010 Limits of quantum speedup in photosynthetic light harvesting. *New J. Phys.* **12**, 065041. (doi:10.1088/1367-2630/12/6/065041)
- 40 Mančal, T. & Valkunas, L. 2010 Exciton dynamics in photosynthetic complexes: excitation by coherent and incoherent light. *New J. Phys.* **12**, 065044. (doi:10.1088/1367-2630/12/6/065044)
- 41 Mančal, T., Balevičius, V. & Valkunas, L. 2011 Decoherence in weakly coupled excitonic complexes. *J. Phys. Chem. A* **115**, 3845–3858. (doi:10.1021/jp108247a)
- 42 Cao, J. & Silbey, R. J. 2009 Optimization of exciton trapping in energy transfer processes. *J. Phys. Chem. A* **113**, 13 825–13 838. (doi:10.1021/jp9032589)
- 43 Wu, J., Liu, F., Shen, Y., Cao, J. & Silbey, R. J. 2010 Efficient energy transfer in light-harvesting systems, I: optimal temperature, reorganization energy and spatial-temporal correlations. *New J. Phys.* **12**, 105012. (doi:10.1088/1367-2630/12/10/105012)
- 44 Tao, G. & Miller, W. H. 2010 Semiclassical description of electronic excitation population transfer in a model photosynthetic system. *J. Phys. Chem. Lett.* **1**, 891–894. (doi:10.1021/jz1000825)

- 45 Huo, P. & Coker, D. F. 2010 Iterative linearized density matrix propagation for modeling coherent excitation energy transfer in photosynthetic light harvesting. *J. Chem. Phys.* **133**, 184108. (doi:10.1063/1.3498901)
- 46 Hossein-Nejad, H. & Scholes, G. D. 2010 Energy transfer, entanglement and decoherence in a molecular dimer interacting with a phonon bath. *New J. Phys.* **12**, 065045. (doi:10.1088/1367-2630/12/6/065045)
- 47 Hayes, D., Panitchayangkoon, G., Fransted, K. A., Caram, J. R., Wen, J., Freed, K. F. & Engel, G. S. 2010 Dynamics of electronic dephasing in the Fenna–Matthews–Olson complex. *New J. Phys.* **12**, 065042. (doi:10.1088/1367-2630/12/6/065042)
- 48 Wilde, M. M., McCracken, J. M. & Mizel, A. 2010 Could light harvesting complexes exhibit non-classical effects at room temperature? *Proc. R. Soc. A* **466**, 1347–1363. (doi:10.1098/rspa.2009.0575)
- 49 Brádler, K., Wilde, M. M., Vinjanampathy, S. & Uskov, D. B. 2010 Identifying the quantum correlations in light-harvesting complexes. *Phys. Rev. A* **82**, 062310. (doi:10.1103/PhysRevA.82.062310)
- 50 Scholak, T., de Melo, F., Wellens, T., Mintert, F. & Buchleitner, A. 2011 Efficient and coherent excitation transfer across disordered molecular networks. *Phys. Rev. E* **83**, 021912. (doi:10.1103/PhysRevE.83.021912)
- 51 Joos, E., Zeh, H. D., Kiefer, C., Giulini, D. J. W., Kupsch, J. & Stamatescu, I.-O. 2003 *Decoherence and the appearance of a classical world in quantum theory*, 2nd edn. Berlin, Germany: Springer.
- 52 Schlosshauer, M. A. 2007 *Decoherence and the quantum-to-classical transition*. Berlin, Germany: Springer.
- 53 Mukamel, S. 1995 *Principles of nonlinear optical spectroscopy*. New York, NY: Oxford University Press.
- 54 Grabert, H., Schramm, P. & Ingold, G.-L. 1988 Quantum Brownian motion: the functional integral approach. *Phys. Rep.* **168**, 115–207. (doi:10.1016/0370-1573(88)90023-3)
- 55 Zurek, W. H. 1991 Decoherence and the transition from quantum to classical. *Phys. Today* **44**, 36–44. (doi:10.1063/1.881293)
- 56 Zurek, W. H. 1992 Preferred states, predictability, classicality and the environment-induced decoherence. *Prog. Theor. Phys.* **89**, 281–312. (doi:10.1143/PTP.89.281)
- 57 Isham, C. J. 1995 *Lectures on quantum theory: mathematical and structural foundations*. London, UK: Imperial College Press.
- 58 Ehrenfest, P. 1927 Bemerkung über die angeneherte Gültigkeit der klassischen Mechanik innerhalb der Quantenmechanik. *Z. Physik* **45**, 455–457. (doi:10.1007/BF01329203)
- 59 Mott, N. F. 1931 On the theory of excitation by collision with heavy particles. *Proc. Cambridge Philos. Soc.* **27**, 553–560. (doi:10.1017/S0305004100009816)
- 60 Billing, G. D. 2003 *The quantum classical theory*. New York, NY: Oxford University Press.
- 61 Haken, H. & Strobl, G. 1973 An exactly solvable model for coherent and incoherent exciton motion. *Z. Physik* **262**, 135–148. (doi:10.1007/BF01399723)
- 62 Leegwater, J. A. 1996 Coherent versus incoherent energy transfer and trapping in photosynthetic antenna complexes. *J. Phys. Chem.* **100**, 14403–14409. (doi:10.1021/jp961448i)
- 63 Gaab, K. M. & Bardeen, C. J. 2004 The effects of connectivity, coherence, and trapping on energy transfer in simple light-harvesting systems studied using the Haken–Strobl model with diagonal disorder. *J. Chem. Phys.* **121**, 7813–7820. (doi:10.1063/1.1786922)
- 64 Wang, H., Song, X., Chandler, D. & Miller, W. H. 1999 Semiclassical study of electronically nonadiabatic dynamics in the condensed-phase: spin–boson problem with Debye spectral density. *J. Chem. Phys.* **110**, 4828–4840. (doi:10.1063/1.478388)
- 65 Adolphs, J. & Renger, T. 2006 How proteins trigger excitation energy transfer in the FMO complex of green sulfur bacteria. *Biophys. J.* **91**, 2778–2797. (doi:10.1529/biophysj.105.079483)
- 66 Wen, J., Zhang, H., Gross, M. L. & Blankenship, R. E. 2009 Membrane orientation of the FMO antenna protein from *Chlorobaculum tepidum* as determined by mass spectrometry-based footprinting. *Proc. Natl Acad. Sci. USA* **106**, 6134–6139. (doi:10.1073/pnas.0901691106)
- 67 Kelly, A. & Rhee, Y. M. 2011 Mixed quantum-classical description of excitation energy transfer in a model Fenna–Matthews–Olsen complex. *J. Phys. Chem. Lett.* **2**, 808–812. (doi:10.1021/jz200059t)

- 68 Kapral, R. & Ciccotti, G. 1999 Mixed quantum-classical dynamics. *J. Chem. Phys.* **110**, 8919–8929. ([doi:10.1063/1.478811](https://doi.org/10.1063/1.478811))
- 69 Kim, H., Nassimi, A. & Kapral, R. 2008 Quantum-classical Liouville dynamics in the mapping basis. *J. Chem. Phys.* **129**, 084102. ([doi:10.1063/1.2971041](https://doi.org/10.1063/1.2971041))
- 70 Nassimi, A., Bonella, S. & Kapral, R. 2010 Analysis of the quantum-classical Liouville equation in the mapping basis. *J. Chem. Phys.* **133**, 134115. ([doi:10.1063/1.3480018](https://doi.org/10.1063/1.3480018))
- 71 Goldsmith, R. & Moerner, W. 2010 Watching conformational and photodynamics of single fluorescent proteins in solution. *Nat. Chem.* **2**, 179–186. ([doi:10.1038/nchem.545](https://doi.org/10.1038/nchem.545))
- 72 Baier, J., Richter, M. F., Cogdell, R. J., Oellerich, S. & Köhler, J. 2008 Determination of the spectral diffusion kernel of a protein by single-molecule spectroscopy. *Phys. Rev. Lett.* **100**, 018108. ([doi:10.1103/PhysRevLett.100.018108](https://doi.org/10.1103/PhysRevLett.100.018108))
- 73 van Dijk, E. M. H. P., Hernando, J., García-López, J.-J., Crego-Calama, M., Reinhoudt, D. N., Kuipers, L., García-Parajó, M. F. & van Hulst, N. F. 2005 Single-molecule pump-probe detection resolves ultrafast pathways in individual and coupled quantum systems. *Phys. Rev. Lett.* **94**, 078302. ([doi:10.1103/PhysRevLett.94.078302](https://doi.org/10.1103/PhysRevLett.94.078302))
- 74 Gerhardt, I., Wrigge, G., Zumofen, G., Hwang, J., Renn, A. & Sandoghdar, V. 2009 Coherent state preparation and observation of Rabi oscillations in a single molecule. *Phys. Rev. A* **79**, 011402. ([doi:10.1103/PhysRevA.79.011402](https://doi.org/10.1103/PhysRevA.79.011402))
- 75 Brinks, D., Stefani, F. D., Kulzer, F., Hildner, R., Taminiau, T. H., Avlasevich, Y., Mullen, K. & van Hulst, N. F. 2010 Visualizing and controlling vibrational wave packets of single molecules. *Nature* **465**, 905–908. ([doi:10.1038/nature09110](https://doi.org/10.1038/nature09110))
- 76 Hildner, R., Brinks, D. & van Hulst, N. F. 2011 Femtosecond coherence and quantum control of single molecules at room temperature. *Nat. Phys.* **7**, 172–177. ([doi:10.1038/nphys1858](https://doi.org/10.1038/nphys1858))
- 77 Scherer, N. F., Carlson, R. J., Matro, A., Du, M., Ruggiero, A. J., Romero-Rochin, V., Cina, J. A., Fleming, G. R. & Rice, S. A. 1991 Fluorescence-detected wave packet interferometry: time resolved molecular spectroscopy with sequences of femtosecond phase-locked pulses. *J. Chem. Phys.* **95**, 1487–1511. ([doi:10.1063/1.461064](https://doi.org/10.1063/1.461064))
- 78 Scherer, N. F., Matro, A., Ziegler, L. D., Du, M., Carlson, R. J., Cina, J. A. & Fleming, G. R. 1992 Fluorescence-detected wave packet interferometry. II. Role of rotations and determination of the susceptibility. *J. Chem. Phys.* **96**, 4180–4194. ([doi:10.1063/1.462837](https://doi.org/10.1063/1.462837))
- 79 Mukamel, S. 1999 *Principles of nonlinear optical spectroscopy*. New York, NY: Oxford University Press.
- 80 Tian, P., Keusters, D., Suzuki, Y. & Warren, W. 2003 Femtosecond phase-coherent two-dimensional spectroscopy. *Science* **300**, 1553. ([doi:10.1126/science.1083433](https://doi.org/10.1126/science.1083433))
- 81 Tekavec, P., Lott, G. & Marcus, A. 2007 Fluorescence-detected two-dimensional electronic coherence spectroscopy by acousto-optic phase modulation. *J. Chem. Phys.* **127**, 214307. ([doi:10.1063/1.2800560](https://doi.org/10.1063/1.2800560))
- 82 Mukamel, S. & Richter, M. 2011 Multidimensional phase-sensitive single-molecule spectroscopy with time-and-frequency-gated fluorescence detection. *Phys. Rev. A* **83**, 013815. ([doi:10.1103/PhysRevA.83.013815](https://doi.org/10.1103/PhysRevA.83.013815))
- 83 Keusters, D., Tan, H. & Warren, W. 1999 Role of pulse phase and direction in two-dimensional optical spectroscopy. *J. Phys. Chem. A* **103**, 10369–10380. ([doi:10.1021/jp992325b](https://doi.org/10.1021/jp992325b))
- 84 Tan, H. 2008 Theory and phase-cycling scheme selection principles of collinear phase coherent multi-dimensional optical spectroscopy. *J. Chem. Phys.* **129**, 124501. ([doi:10.1063/1.2978381](https://doi.org/10.1063/1.2978381))
- 85 Myers, J., Lewis, K., Tekavec, P. & Ogilvie, J. 2008 Two-color two-dimensional Fourier transform electronic spectroscopy with a pulse-shaper. *Optics Exp.* **16**, 17420–17428. ([doi:10.1364/OE.16.017420](https://doi.org/10.1364/OE.16.017420))
- 86 Shim, S. & Zanni, M. 2008 How to turn your pump-probe instrument into a multidimensional spectrometer: 2D IR and Vis spectroscopies via pulse shaping. *Phys. Chem. Chem. Phys.* **11**, 748–761. ([doi:10.1039/b813817f](https://doi.org/10.1039/b813817f))
- 87 Gundogdu, K., Stone, K., Turner, D. & Nelson, K. 2007 Multidimensional coherent spectroscopy made easy. *Chem. Phys.* **341**, 89–94. ([doi:10.1016/j.chemphys.2007.06.027](https://doi.org/10.1016/j.chemphys.2007.06.027))
- 88 Dawlaty, J., Bennett, D., Huxter, V. & Fleming, G. R. 2011 Mapping the spatial overlap of excitons in a photosynthetic complex via coherent nonlinear frequency generation. *J. Chem. Phys.* **135**, 044201. ([doi:10.1063/1.3607236](https://doi.org/10.1063/1.3607236))